Investigating an analytic model for neutrino light curves of core-collapse supernovae

ASIoP Summer Student Program

2023 Final Presentation & Poster Exhibition

Chang-Mao Yang[1,*] supervised by Manu George[2] and Meng-Ru Wu[2] (*409220055@alum.ccu.edu.tw)

[1]*Department of Physics, National Chung Cheng University* [2]*Institute of Physics, Academia Sinica*

Abstract:

In this study, we introduce a model to characterize the neutrino light-curve following a core-collapse supernova event. Our model differentiates between the early and late phases of post-neutrino star (PNS) cooling, offering insights into neutrino behaviors and interactions. From the numerical simulation, we determine the PNS radius using two methods: the location with the steepest density change and the location of zero radial velocity. To extract the four parameters not directly obtained from simulations, we employ non-linear least square fitting. We then compare our model's predictions with numerical simulations, with a focus on the neutrino luminosity and mean energy. The findings suggest that the parameters have a significant impact on the luminosity. While the light curve fitting results are promising, the predictions for mean energy are less optimal. As such, further validation and more extensive numerical comparisons are anticipated in future work.

Introduction:

Supernovae, resulting from the core collapse of massive stars, are the universe's grand explosions. Central to this are neutrinos, tiny particles that carry away energy, shape the explosion, and offer a window into these events. The main stages include:

1. **Core Collapse**: Star's core turns to iron, collapsing and emitting neutrinos.
2. **Neutrino Trapping**: Increasing core density traps these neutrinos.
3. **Shock Formation**: The core sudden compression creates a shock wave that moves outward.
4. **Neutrino Burst**: As the outward shock wave decreases in density, it allows the trapped neutrinos to burst out, leading to a bright electron neutrino burst and the production of neutrinos of all flavors.
5. **Shock Revival**: Neutrinos give a boost to the stalled shock wave, delivering a successful explosion, leaving behind a PNS.
6. **Cooling & Wind**: The forming star cools, releasing neutrinos that drive a unique wind, potentially crafting trans-iron elements.

Our research focuses on the neutrino light curve produced during the last cooling phase of the proto-neutron star (PNS). As the outward shock propagates, it evolves over decades to millennia, eventually forming a supernova remnant, as shown in FIG. (1).

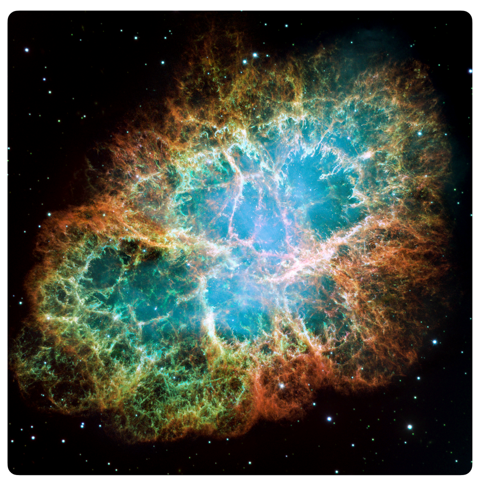

FIG. (1) The Crab Nebula, a supernova remnant resulting from a core-collapse supernova explosion. Image courtesy of NASA/ESA Hubble Space Telescope.

Neutrino Light-Curve Model:

Based on Ref. [1]'s method, we describe the distribution function of neutrinos, $f = f(t, r, \mu, E)$, using the Boltzmann transport equation up to order $\mathcal{O}(v/c)$. The equation is given by

$$\frac{df}{cdt} + \mu\frac{\partial f}{\partial r} + \left[\mu\left(\frac{d\ln\rho}{cdt} + \frac{3v}{cr}\right) + \frac{1}{r}\right](1-\mu^2)\frac{\partial f}{\partial \mu} + \left[\mu^2\left(\frac{d\ln\rho}{cdt} + \frac{3v}{cr}\right) - \frac{v}{cr}\right]E\frac{\partial f}{\partial E}$$
$$= j(1-f) - \chi f + \frac{E^2}{c(hc)^3}\left[(1-f)\int Rf'\,d\mu' - f\int R(1-f')\,d\mu'\right]$$

where μ represents the cosine of the angle between the radial direction and neutrino propagation. E is the neutrino energy, v denotes the fluid velocity relative to the laboratory frame, c is the speed of light, j is the emissivity, χ is the absorptivity, and R is the isoenergetic scattering kernel. By applying the Lane-Emden equation solution for $n = 1$ near the PNS surface, we derive the neutrino light-curve as

$$L = 3.3\times 10^{51}\,\mathrm{erg}\cdot\mathrm{s}^{-1}\left(\frac{M_{\mathrm{PNS}}}{1.4\,M_\odot}\right)^{6}\left(\frac{R_{\mathrm{PNS}}}{10\,\mathrm{km}}\right)^{-6}\left(\frac{g\beta}{3}\right)^{-4}\left(\frac{t+t_0}{100\,\mathrm{s}}\right)^{-6}$$

and the mean energy as

$$\langle E_\nu\rangle = 16\,\mathrm{MeV}\left(\frac{M_{\mathrm{PNS}}}{1.4\,M_\odot}\right)^{3/2}\left(\frac{R_{\mathrm{PNS}}}{10\,\mathrm{km}}\right)^{-2}\left(\frac{g\beta}{3}\right)\left(\frac{t+t_0}{100\mathrm{s}}\right)^{-3/2}.$$

In these equations, M_{PNS} and R_{PNS} represent the mass and radius of the PNS, respectively. β is a dimensionless factor that boosts scattering due to the presence of heavy nuclei (with $\beta \approx 3$ for free nucleons). g is a dimensionless parameter accounting for the different structure of the PNS surface. The t_0 is given by

$$t_0 = 210\,\mathrm{s}\left(\frac{M_{\mathrm{PNS}}}{1.4\,M_\odot}\right)^{6/5}\left(\frac{R_{\mathrm{PNS}}}{10\,\mathrm{km}}\right)^{-6/5}\left(\frac{g\beta}{3}\right)^{4/5}\left(\frac{E_{\mathrm{tot}}}{10^{52}\,\mathrm{erg}}\right)^{-1/5}.$$

As the PNS cools, β changes, influencing the neutrino light curve. Adapting from Ref. [1], we model this with two phases: early without coherent scattering ($\beta \approx 3$) and later with increased opacity ($\beta \gg 1$). We then combine their luminosities and mean energies to be

$$L = L_1 + L_2,\quad \langle E_\nu\rangle = \frac{L_1 + L_2}{L_1/\langle E_{\nu,1}\rangle + L_2/\langle E_{\nu,2}\rangle}$$

With these analytic solutions in hand, we can proceed to extract parameters from observed data. However, before doing so, we first compare our model with numerical simulations.

Numerical Comparison and Analysis:

We take simulation data from Ref. [2], obtaining various physical quantities over time, such as radius r, density ρ, velocity v, internal mass m, and more. For our model, the PNS radius and mass are crucial. We define the PNS radius using two methods:

1. **Density Gradient:** The location with the steepest change in density.
2. **Velocity Transition:** The boundary where material motion switches from inward to outward, i.e., $v = 0$.

From the data, we then determine the mass enclosed within the defined PNS radius. Our model distinguishes between early and late phases. We split β into $\beta_1 = 3$ for the early phase and $\beta_2 \gg 1$ for the late phase. Additionally, we divide the total energy due to different thermal mechanisms into $E_{\mathrm{tot},1}$ and $E_{\mathrm{tot},2}$. This gives us four parameters need to be determined: $\beta_2, E_{\mathrm{tot},1}, E_{\mathrm{tot},2}$ and g, a free parameter for the PNS surface structure.

Taking a specific simulation run as an example, we present the results for the radius and mass of the PNS in the following table.

Definition	R_{PNS} (km)	M_{PNS} ($M_\odot$)
Density Gradient	14.01	1.574
Velocity Transition	15.65	1.581

Utilizing the non-linear least square method over a chosen time interval near 1s to 10s, we determine the value of $\beta_2, E_{\mathrm{tot},1}, E_{\mathrm{tot},2}$ and g. By comparing the fit of the resulting curves to the simulation data, we can assess the model's validity and applicability.

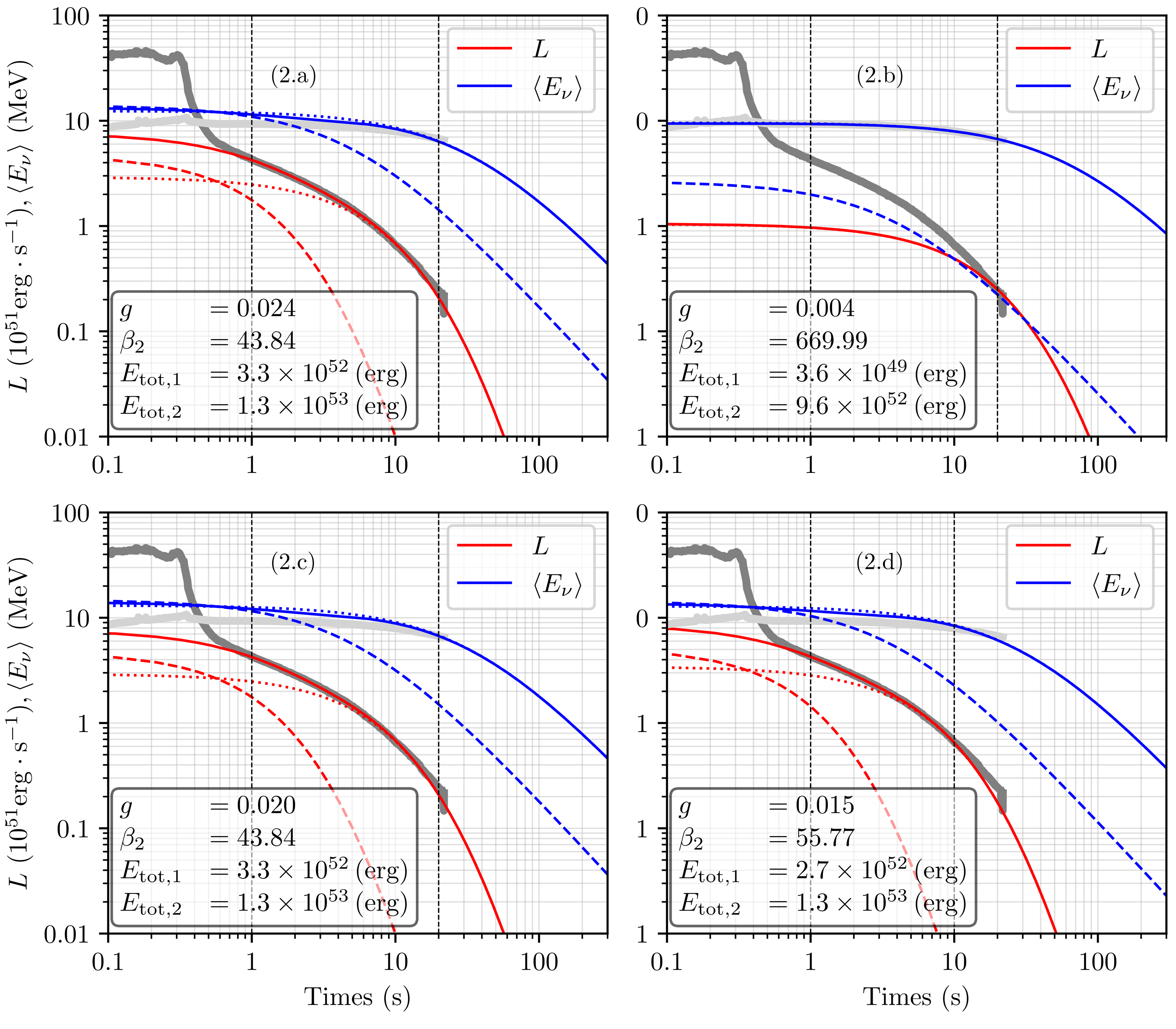

FIG. (2) In the figures, the dashed lines represent the early phase, while the dotted lines indicate the late phase. The solid lines show the total, and the grey lines correspond to the simulation data.
(2.a): Luminosity fitting using Velocity Transition-defined PNS radius (1s ~ 20s).
(2.b): Mean energy fitting with Velocity Transition-defined PNS radius (1s ~ 20s).
(2.c): Luminosity fitting with Density Gradient-defined PNS radius (1s ~ 20s).
(2.d): Luminosity fitting with Velocity Transition-defined PNS radius (1s ~ 10s).

Results and Discussion:

From the four figures in FIG(2), we can observe the following points:

1. **L's Sensitivity:** The L fitting in FIG (2.a) showed a more consistent and reliable fit compared to the $\langle E_\nu\rangle$ in FIG (2.b). This suggests that our model's parameters are sensitive to changes in L.
2. **Consistency Across PNS Definitions**: The L fit remained largely consistent when we altered the definition of the PNS radius, as seen when comparing FIG (2.a) and (2.c). This suggests that the model is not significantly affected by different definitions of the PNS radius.
3. **Effect of Time Range:** Even when the time range was shortened to 1s ~ 10s in FIG (2.d), the L fit remained satisfactory, showcasing the model's adaptability.
4. **$\langle E_\nu\rangle$ Fitting Challenges:** Despite achieving good fits for L, the $\langle E_\nu\rangle$ curves were less ideal. This difference underscores potential areas of improvement in our model's treatment of $\langle E_\nu\rangle$.

In summary, our model aligns well with the L curve. In the future, we plan to compare with more numerical simulation results and explore other methods to validate the reliability of this model, such as examining the Equation of State for the PNS and so on.

Reference:

[1] Y. Suwa et al., 2021, "Analytic solutions for neutrino-light curves of core-collapse supernovae," Prog. Theor. Exp. Phys., 013E01. DOI: 10.1093/ptep/ptaa154
[2] T. Fischer et al., 2010, "Protoneutron star evolution and the neutrino-driven wind in general relativistic neutrino radiation hydrodynamics simulations," A&A, vol. 517, A80. DOI: 10.1051/0004-6361/200913106
[3] K. Sumiyoshi et al., 2017, "Neutrino Emissions up to the Pre-bounce of Massive Stars," arXiv:1702.08713 [astro-ph.HE].